Available online at www.sciencedirect.com
SCIENCE DIRECT®
Journal of Hydrology 275 (2003) 109–121
Journal of Hydrology
www.elsevier.com/locate/jhydrol

Assessment of direct transfer and resuspension of particles during turbid floods at a karstic spring

N. Massei[a,*], H.Q. Wang[a,b], J.P. Dupont[a], J. Rodet[a], B. Laignel[a]

[a]*Département de Géologie, Université de Rouen, UMR CNRS 6143 M2C, 10, Boulevard de Broglie, 76821 Mont-Saint-Aignan cedex, France*
[b]*Laboratoire de Mécanique, Université du Havre, 76600 Le Havre, France*

Received 22 July 2002; accepted 7 January 2003

Abstract

Turbid water can be the source of important sanitary problems in karstic regions. It is the case of the Pays de Caux, in Haute Normandie, where the main resource in drinking water is provided by the chalk aquifer. In the case of the typical binary karst of the Pays de Caux, turbidity results from the input in sinkholes of turbid surface water induced by erosion on the plateaus. At some spring tappings, water may be very turbid in period of intense rainfall. The turbidity observed at a karstic spring is a complex signal which contains a part of direct transfer and a part of resuspension of the particles being transported. The aim of this study is turbidigraph separation, which would permit to distinguish the direct transfer and resuspension components of the turbidigraph. These two components are separated by comparing the elementary surface storm-derived water fluxes and elementary turbidity signals at the spring. The procedure takes place in three phases: (i) spring hydrograph separation by means of a two components mixing model (surface water and karstic groundwater) using specific electrical conductivity, (ii) decomposition of storm-derived water flux and turbidity thanks to the second-derivative method, (iii) comparison of the transfer times (≈modal times) of the elementary turbidity and surface water flux signals, respectively. The mass corresponding to direct transfer, computed after signal decomposition, is then used to re-calculate a particle recovery rate, which passes so from 51 ± 4 to 37 ± 3%. Relations between particle flux and hydrodynamics show that resuspension can be either the fact of the dynamics of the introduction system, or that of the chalk karstic aquifer in general (case of resuspension not associated to surface water flux). In this sense, evolution of particle flux (and consequently of turbidity) can be also a marker of the karst structure.

Keywords: Karst; Electrical conductivity; Turbidity; Resuspension; Direct transfer; Turbidigraph separation

1. Introduction

Suspended sediment plays an important role in the contamination of karst aquifers and potable water because of the ability of bacteria to sorb onto particulates. Several studies have demonstrated the increased survival of microorganisms when they are associated with particulates (Palmateer et al., 1993; Pommepuy et al., 1992); particulates are thus potential vectors of microbial contamination. The transport of particulates and the associated risks for public health in areas where drinking water comes

* Corresponding author. Tel.: +33-0-235-146-730; fax: +33-0-235-147-022.
E-mail address: nicolas.massei@univ-rouen.fr (N. Massei).

0022-1694/03/$ - see front matter © 2003 Elsevier Science B.V. All rights reserved.
doi:10.1016/S0022-1694(03)00020-9

from karst aquifers has come under scrutiny over the last several years. In Haute-Normandie, where virtually 100% of the groundwater resources are provided by karst aquifers, suspended particulates have a non-negligible influence on public health (Beaudeau et al., 1999). At karstic springs, the problem is generally correlated with high turbidity associated with heavy rainfall periods.

The transport of supra-micrometric particles in karstic media is a complex process implying deposition and release phenomena (Massei, 2001). Hence, at the flood scale, the observed turbidity would have two potential origins: (i) an allochthonous origin corresponding to the direct transfer of particulate materials from the inlet to the outlet of the karstic system, and (ii) a resuspended origin, which is related to resuspension of previously deposited sediment within the karstic network. Actually, when comparison is made of the mass swallowed in a sinkhole and the mass recovered to a spring (Massei, 2001), the occurrence of particle release can lead to an important overestimation of the mass balance (apparent recovery rate at the spring).

The transport of the liquid phase in karstic aquifers is relatively well known by means of hydrogeochemistry (Bakalowicz, 1979), which constitutes for a long time a powerful tool for hydrograph separation. Recent studies contribute also to increase the accuracy of models and consequently the knowledge of karst functioning (Pinault et al., 2001; Plagnes, 1997). For particle transport, the main difficulty is linked to the distinction between the autochthonous (resuspended) and the allochtonous part of turbidity during a flood. For instance, particle markers usually lack for characterizing the origin of turbidity. The tracing of tagged particles has been undertaken, notably by Mahler et al. (1998a,b)). Nowadays, the most frequently used in situ methodologies are based on geochemistry (Mahler and Lynch, 1999; Mahler et al., 1999; Vaute et al., 1997; Wicks and Engeln, 1997), but analysis of particle size distribution has also been shown to be useful (Lacroix et al., 1998, 2000). Studies of the properties of stocking and release of sediment in karstic media were also carried out (Coquerel et al., 1993; Lacroix et al., 1998; Mahler and Lynch, 1999; Rodet, 1991, 1993, 1996). In most cases, these studies concern the identification of sedimentary stocks with specific physical properties: well-sorted particles of specific size or mineralogical compositions according to their origin, etc.

In our case, intra-karstic sedimentation results from a decrease in flow competence: this phenomenon usually appears as flow paths widen in the karstic network (e.g. from small conduits to larger zones such as large cavities or conduits). The decrease in velocity allows particles to settle. These particles may be resuspended later and transported by subsequent high-competence flow events and have similar physical and mineralogical patterns, both autochthonous resuspended and allochthonous particles originating from soil erosion.

2. Study site and methods

2.1. Geomorphological and hydrogeological setting

The Norman climate is typically oceanic. Average temperatures are of the order of 10–12 °C and annual average precipitation vary between 600 and 1100 mm.

On a morphological point of view, the Pays de Caux is characterized by chalk plateaus covered with clay-with-flints owing to chalk weathering (Laignel et al., 1999, 2002a,b). These clay layers are themselves covered with quaternary silts (Lautridou, 1985). On the right side of the Seine river, the Pays de Caux has a maximal height of 243 m. The clay-with-flints constitutes a fairly impervious layer that covers the chalk. It locally penetrates the chalk through the above-mentioned impervious layer, resulting in a strong connection of the surface with the aquifer. Plateaus are situated on the sides of the lower Seine valley, which is filled by holocene alluvial deposits.

The Norville karstic system is located on the right side of the river Seine, about 40 km away from the Seine estuary (Fig. 1(a)). This kind of system is typical of the karst of the lower Seine valley (Fig. 1(b)). The Norville system has been widely studied and its boundaries became quite well known (Massei, 2001; Massei et al., 2002). It is constituted of a sinkhole on the plateau, where surface runoff waters of a creek named ‘Bébec’ are swallowed, and of a spring at the base of the plateau, at the place named ‘Le Hannetôt’. This spring constitutes an overflow of

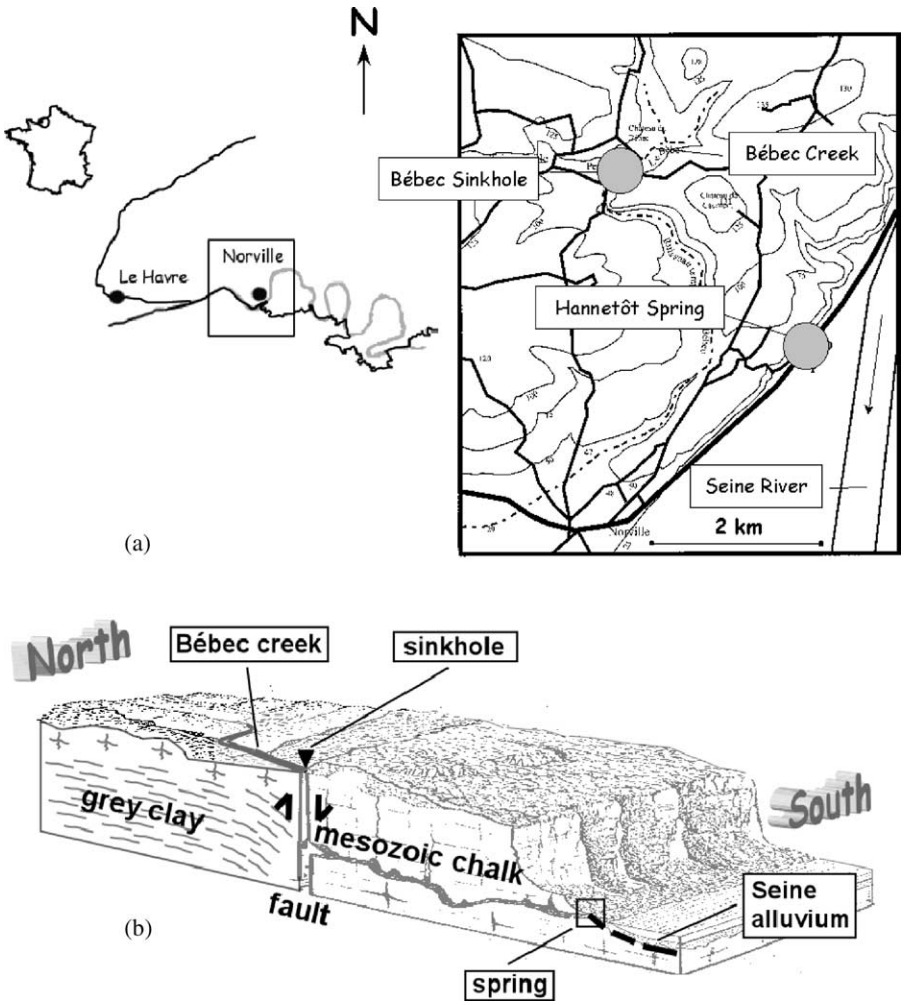

Fig. 1. (a) Location of the study site; (b) geomorphologic setting (Massei et al., 2002).

the saturated zone. It is a barrier spring resulting from the fine semi-permeable alluvial deposits covering the chalk aquifer in the Seine valley.

During major rain events, turbid water of Bébec creek resulting from soil erosion is introduced into the sinkhole. The Hannetôt spring is clearly identified as being the main outlet of waters swallowed in the sinkhole.

2.2. Methods

Field equipment is constituted by multi-parameters 6820 YSI datasonds, each comprising one turbidity probe, one electrical conductivity probe, and one pressure sensor. Each datasond is connected to an ISCO 6700 automatic sampler, which allows, besides the sampling, the recording of all the measured parameters. Datasonds are calibrated and controlled by means of the EcoWatch software (YSI INC.). An ISCO 674 rain gauge is settled on the watershed. Spring discharge is measured according to a 15 min time step with an ISCO 4150 Doppler flowmeter. Turbidity, electrical conductivity and precipitation are also recorded according to a 15 min time step. Data are downloaded by means of the ISCO Flowlink 3 software (ISCO INC.).

2.3. Natural tracer and dye tracer tests

The Hannetôt spring has been the object for several years of a continuous recording of turbidity, electrical conductivity and discharge (Massei, 2001). The distribution of electrical conductivity frequencies, as described by Bakalowicz (1979), can be used to give evidence of the karstic character of this system (Fig. 2): such a multi-modal and spreaded distribution is linked to a strong variability of water chemistry at the karstic spring throughout the year. Several types of water can be distinguished, demonstrating a quite complex karstic system. One should notice (i) higher frequencies and mineralization for chalk matricial water typical of no-rainy and dry periods, (ii) intermediate frequencies and mineralization for karstic response to recharge and diffuse infiltration, and (iii) lower frequencies and mineralization related to the occurrence at the spring of storm-derived water consequently to rain events.

Several tracer tests were realized during the last three years, each one being performed during no rainfall periods, either in dry or wet seasons. They are represented in Fig. 3(a) as residence time distributions. This type of representation is classically used for the comparison of tracing: information about the apparent transfer velocity remains available and breakthrough curves can be compared using the same graph, their area being normalized. The obtained transfer time is variable, from 16 to 29 h.

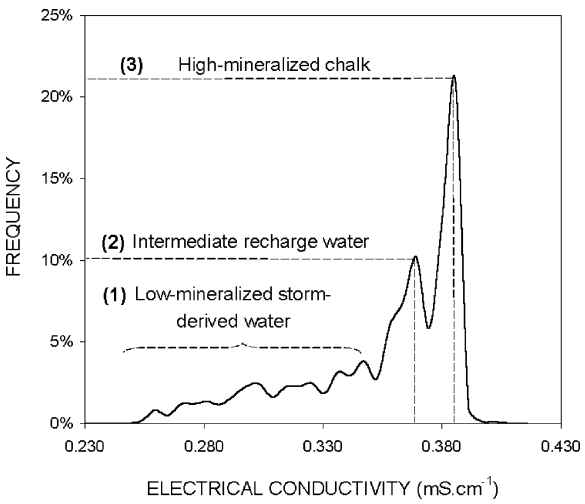

Fig. 2. Distribution of electrical conductivity frequencies. This multi-modal distribution shows (1) typically high-mineralized chalk porosity groundwater, (2) low-mineralized storm-derived water, (3) intermediate water originating from recharge, all types of water being drained by the karstic network. The electrical conductivity values presented here correspond to a one-year survey (January 2000–January 2001).

Residence time distribution is a useful representation for the comparison of tracer tests, especially if the recovered masses of tracer are very different: peak area is always equal to one.

A second representation allows to compare graphically the tracer breakthrough curves. This representation is independent of the flow-rate. This method consists in normalizing both the tracer flux and the time. The normalized tracer flux is:

$$\varphi_N = \frac{\varphi_i \Delta t}{M} \tag{1}$$

where φ_i is the tracer flux during Δt, and M the mass recovered. The normalized time t_N is obtained from $t_N = t/t_m$, where t is the time since input and t_m the mean transit time, that is:

$$t_m = \frac{\int_0^{+\infty} C(t)Q(t)t \, dt}{\int_0^{+\infty} C(t)Q(t) \, dt} \tag{2}$$

or in its discrete form:

$$t_m = \frac{\sum_{i=1}^{N} C_i Q_i t_i}{\sum_{i=1}^{N} C_i Q_i} \tag{3}$$

with t, C, Q: time since input, concentration and spring discharge.

Then, the spreading and asymmetry of the breakthrough curves can be easily compared, and their surface gives the recovery rate (Fig. 3(b)). The breakthrough curves are almost centered on 1, but modal time is always slightly lower than the mean time because of the asymmetry of the curves. The variances of the normalized breakthrough curves show a slight decrease with increasing flow-rate. The dispersivity values associated to each tracer test have been calculated thanks to the Qtracer2 program (Field, 2002 #549), which uses the Chatwin method (Chatwin, 1971 #555) for longitudinal dispersion calculation. Dispersivities are provided in Table 1

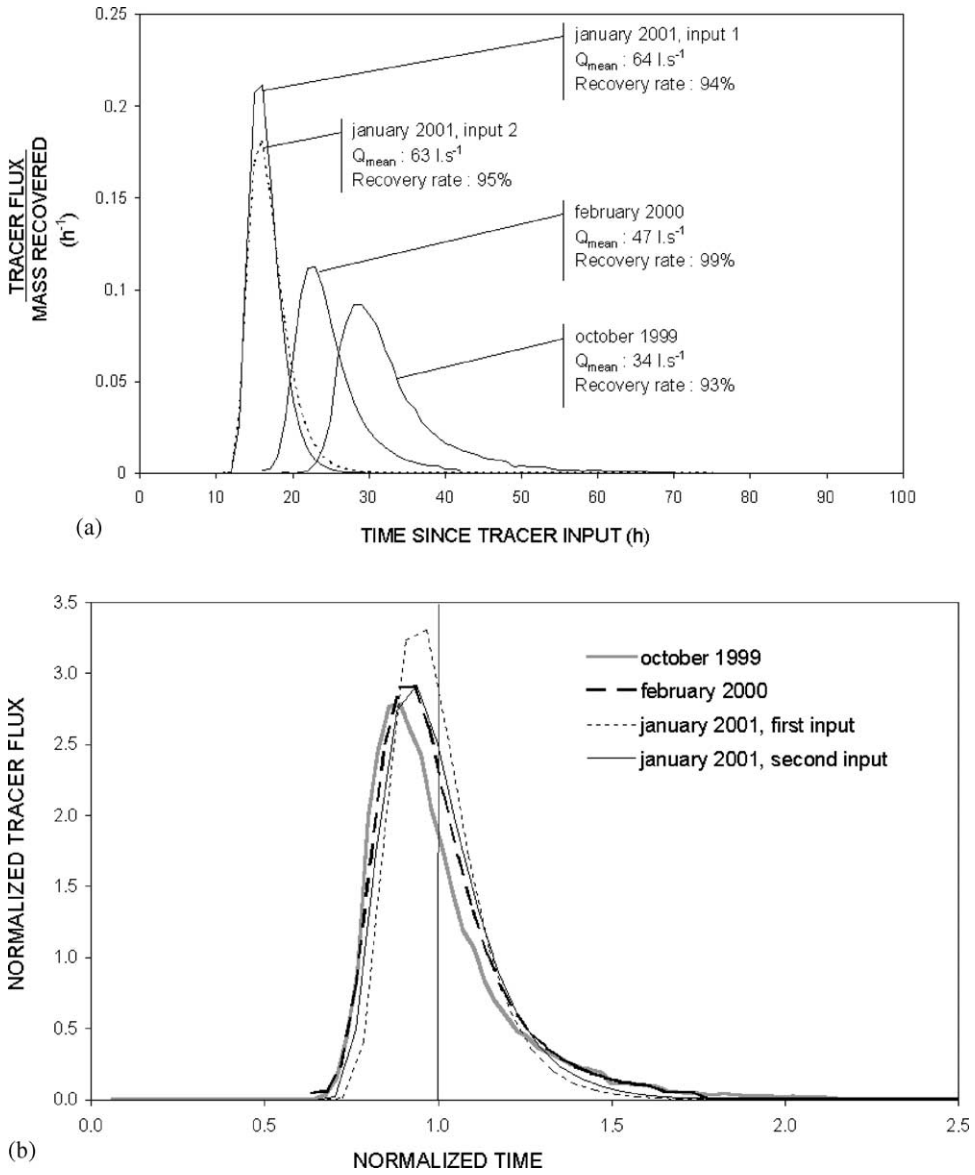

Fig. 3. (a) Residence times distributions for four dye tracer tests. Spring discharge remained fairly constant and no rainfall occurred during each test. Area of each curve equals one; (b) normalized tracer breakthrough curves at the spring. The area of each curve gives the corresponding recovery rate.

with variance values. Dispersivity tend to decrease with flow-rate, as it was observed for variance. The dispersivity values are of the order of 12–20 m.

Hence, the Norville system presents typical karstic characteristics, with important apparent transfer velocities. The recovery rates of the tracer are strong. The unimodal shape of the breakthrough curves and the high apparent transfer velocities allow to consider the system as a main conduit accounting for the major part of the surface stream introduced in the sinkhole. The volume V_m of the main conduit system can be estimated according to the relation:

$$V_m = Q_m t_m \quad (4)$$

Table 1
Measured data and calculated parameters for dissolved tracer and particulate

Period of the tracer test	October 1999	February 2000	January 2001 (1)	January 2001 (2)
Mean Spring discharge ($l\,s^{-1}$)	34	47	64	63
Mean transit time t_m (h)	32.6	23.6	16.5	17.0
Mean apparent transfer velocity ($m\,h^{-1}$)	67.5	93.2	133.3	129.4
Volume of main conduit (m^3)	3.996×10^3	3.970×10^3	3.801×10^3	3.855×10^3
Tracer recovery rate (%)	93	99	94	95
Variance of the normalized breakthrough curves	0.59	0.59	0.49	0.44
Dispersivity (m)	19.7	18.9	12.7	12.9

where Q_m and t_m are the mean discharge and transit time, respectively. The obtained volume is of the order of 4000 m^3. This volume remains fairly constant whatever flow rate. Data relative to various dye tracings are summarized in Table 1.

3. Water and particle discharge at the spring during one flood

3.1. Spring response to rainfall

Three rain or storm events were sampled from December 1999 (Massei et al., 2002) to November 2000. Several other events were monitored during the same period. Each one showed typical characteristics with respect to turbidity occurrence at the spring: a fast response with lags (modal concentration at the sinkhole/modal concentration at the spring) typical of conduit-flow velocities.

We base our analysis on one example of flood event which occurred April 2000. This turbid event was chosen, as it was quite representative of the typical turbid response of the system. Moreover, it has the advantage of being a fairly isolated episode, which allows to clearly distinguish the beginning and the end of the flood. Actually several events consist of multiple (>2) rain pulses or storms and induce multi-modal turbidity responses over long periods (>1 week). Turbidity, discharge and electrical conductivity are recorded at Bébec sinkhole and Hannetôt spring. Fig. 4(a) and (b) present raw data recorded at Hannetôt spring.

Throughout the period, cumulative rainfall is of 17.36 mm. However, only the first rain pulses (from 14/04 6.30 PM to 15/04 10.45 PM) are related to the turbid flood recorded at the spring. These pulses amount to 12.95 mm and can be separated in 2 phases R1 (7.97 mm) and R2 (4.97 mm).

The first observations show that particle flux do not seem directly correlated to spring discharge (Fig. 4(a)). We can also notice the increase of spring discharge at the end of the turbid event without any clear relation with precipitation. On the other hand, the evolution of the electrical conductivity seems to be linked to that of particle breakthrough (Fig. 4(b)). As a first approach, if one considers the decreasing conductivity as a surface water flux indicator at the spring, particle flux observed at the spring would occur consequently to turbid surface water at the sinkhole.

The recording of particle fluxes at both sinkhole and spring permits us to compute the total recovered mass at the spring during the flood, which is $3.22 \pm 0.14 \times 10^2$ kg. It is now recognized on this site—as in most cases—that all the recovered mass does not correspond to direct transport through the system: deposition and release phenomena can be important (Massei, 2001). The main difficulty consists in trying to quantify these phenomena from recorded data.

3.2. Spring hydrograph separation

For spring hydrograph separation we used a simple two-component mixing model: (i) a surface component Q_{Stw} (storm-derived water swallowed in the sinkhole), and (ii) a karst component Q_{Aq} characterizing spring discharge in absence of rainfall. Hydrograph separation is realized by means of electrical conductivity, recorded with a 15 min time step at both sinkhole and spring. This parameter presents indeed

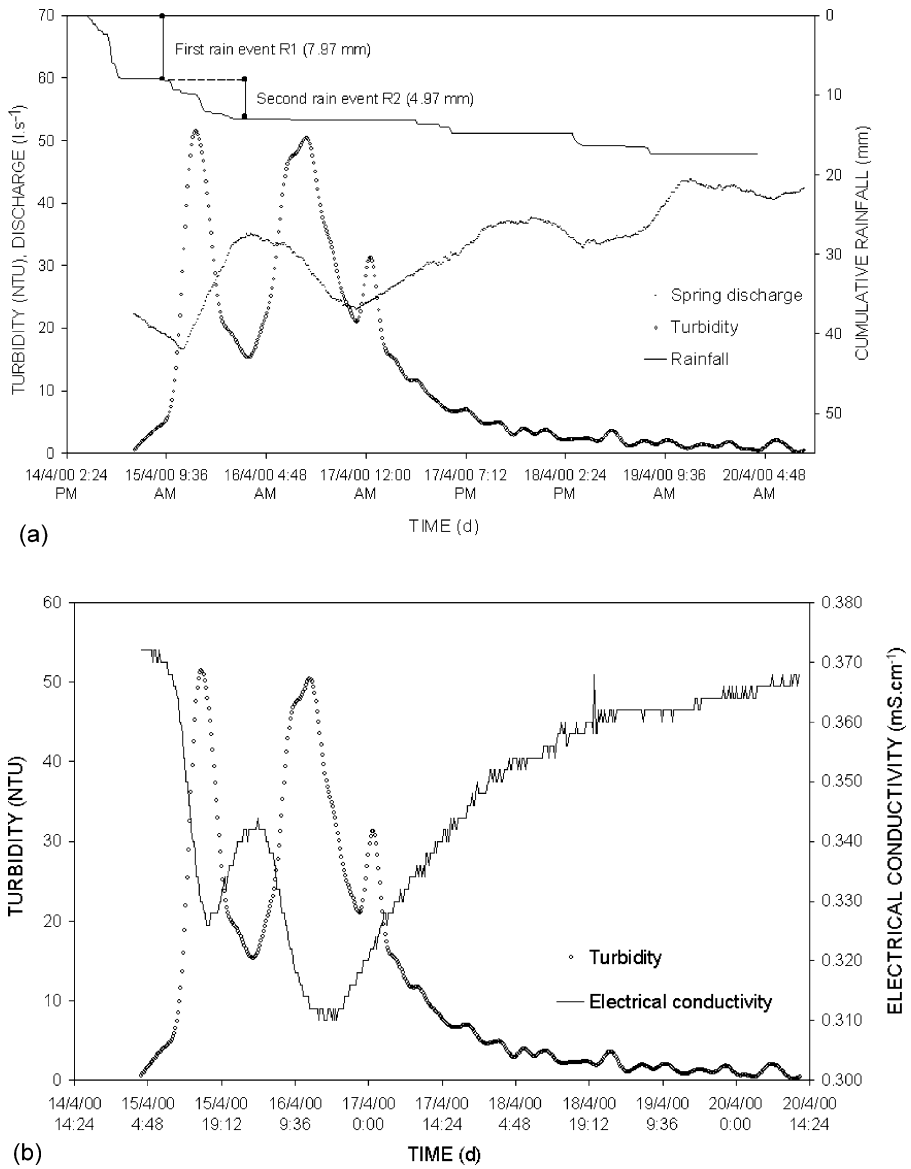

Fig. 4. Raw data recorded at the Hannetôt spring during the 14 April flood: (a) rainfall, total spring discharge and turbidity; (b) electrical conductivity and turbidity.

the advantage to be easily measurable in situ. Moreover, in the case of such binary karstic systems, the high contrast in electrical conductivity between groundwater and storm-derived water allows to use this parameter as a good indicator of surface water arrival at the spring. The variations at the spring of the electrical conductivity can be used in first approach to quantify the contribution of storm-derived water to total spring discharge. At the spring, the instantaneous discharge measured every 15 min is given by:

$$Q_S = Q_{Aq} + Q_{Stw} \quad (5)$$

Also, the instantaneous flux of dissolved ionic species (measured indirectly by means of the electrical

conductivity every 15 min) is:

$$Q_S C_S = Q_{Aq} C_{Aq} + Q_{Stw} C_{SH} \quad (6)$$

Where Q_S is the total spring discharge, Q_{Aq} the karstic component of spring discharge, Q_{Stw} the surface component of the spring discharge (storm-derived water flux contribution to total spring discharge), C_S the recorded specificelectrical conductivity at the spring (25 °C—compensated electrical conductivity), C_{SH} the recorded specific electrical conductivity (25 °C—compensated) of surface water swallowed in the Bébec sinkhole, which variations are related to runoff, and C_{Aq} (constant) the electrical conductivity at the spring during dry periods.

Solving of Eqs. (4) and (5) gives:

$$Q_{Aq} = Q_S \frac{(C_S - C_{SH})}{(C_{Aq} - C_{SH})} \quad (7)$$

$$Q_{Stw} = Q_S \frac{(C_S - C_{Aq})}{(C_{SH} - C_{Aq})} \quad (8)$$

At the maximum of the surface water flux, the contribution to the total discharge is 42%.

Hydrograph separation, graphically presented in Fig. 5, allows to sharply distinguish the fast response of the storm-derived component, which gives an apparent velocity typical of conduit flow systems (≈ 160 m h^{-1}), as highlighted both artificial tracer tests and natural tracer. Hydrograph separation also illustrates more precisely the relations between spring hydrodynamics and turbidity (Fig. 6), which was not obvious by only comparing total spring discharge and turbid response.

Finally, the variations of the aquifer component of spring discharge can be also distinguished. The increase of karst aquifer discharge appears about 20 h after the beginning of the rain, which corresponds to a rather short response time. These variations express the aquifer's response in its entirety under the effect of recharge. This fast and rather complex response would demonstrate (i) a strong hydraulic connection between surface (plateaus) and groundwater in terms of aquifer recharge, (ii) a fairly complex karstic structure of the saturated zone, involving strong displacements of water. This last point has been attested by the distribution of electrical conductivities.

3.3. Peak detection and fitting applied to storm-derived water and particle breakthrough at the spring

We can try to deepen the analysis of particle transport by decomposing (i) the surface component of spring discharge, and (ii) the particle flux

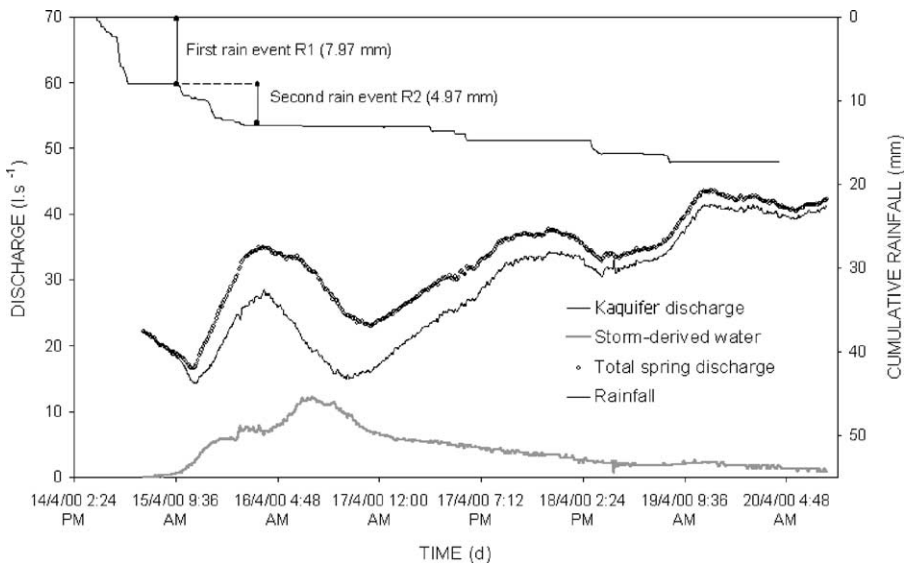

Fig. 5. Total, karst and storm-derived water discharge at the spring during the flood determined by means of electrical conductivity-based hydrograph separation.

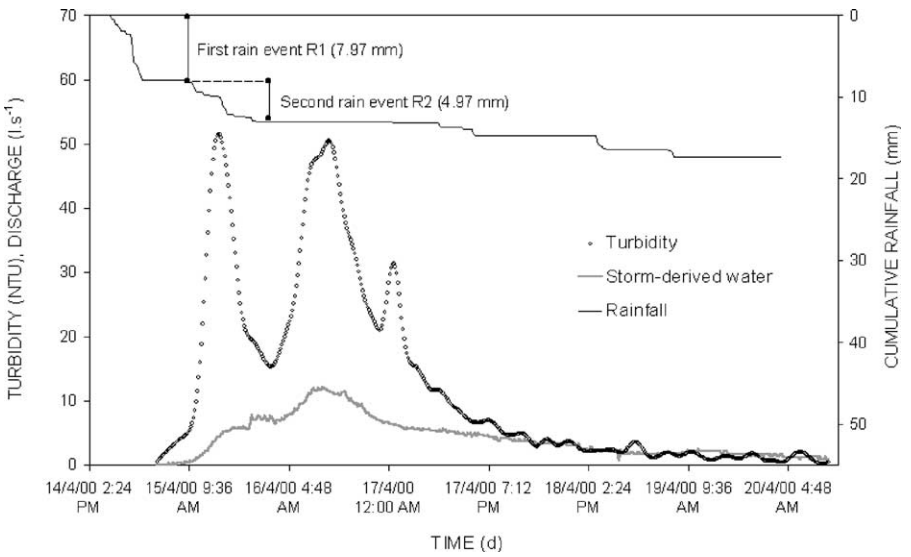

Fig. 6. Storm-derived water component and turbidity at the spring.

breakthrough curve. We used for that the signal processing software PeakFit (SPSS INC.). The purpose of such an approach is to define the relations between elementary particle breakthrough curves and storm-derived water flux at the spring in terms of transfer time, so as to distinguish the resuspended part (intrakarstic resuspension) from the allochthonous part (direct transfer) of particle flux for the considered flood. Peak detection is realized using the second-derivative method: visible peaks are defined as those which produce local maxima in the input data, whereas hidden peaks, defined as those which fail to produce local maxima, are detected by second derivative minima. Breakthrough curves of artificial tracer being well represented with log–normal curves with coefficient of asymmetry of 1.5, we used this latter type for the decomposition of both surface water flux and particle breakthrough curves.

For surface water flux at the spring, 4 main peaks can be distinguished (Fig. 7(a)), explaining 99% of the total signal. These peaks are labelled Q_{S1}, Q_{S2}, Q_{S3}, and Q_{S4}. The total turbidity signal also shows several local maxima. We use the same method for signal decomposition into a linear combination of elementary turbidity signals T_{Si}. In this case, six elementary signals (e.g. T_{S1}, T_{S2}, T_{S3}, T_{S4}, T_{S5} and T_{S6}) explain 98% of the total curve (Fig. 7(b)). The number of peaks used for the decomposition has been chosen to obtain the best fit of the total signal, but has been limited as much as possible to the variations that we thought significant. For each T_{Si}, the recording of spring discharge allows to calculate a corresponding recovered mass.

Comparison is made of the various particle and surface flux peaks according to their modal time. Actually, the modal time appears to be the most representative value for convective transport estimation: storm-derived water and turbidity elementary peaks that have similar modal time (e.g. transfer time) can be related. Corresponding particle breakthrough curves would be due to transport by surface water fluxes (direct transfer). Otherwise, elementary particle peaks should be associated with resuspension of previously deposited sediment. According to this, we can correlate Q_{S1} with T_{S2}, Q_{S2} with T_{S3}, and Q_{S3} with T_{S4}. Moreover, it appears that some T_{Si} peaks cannot be correlated with any Q_{Si} peaks: T_{S1}, T_{S5} and T_{S6} cannot be associated to surface fluxes.

3.4. Direct transfer, resuspension and implications on karst functioning

The measurements realized at the sinkhole (total mass of particulate material swallowed) allow to calculate a mass-balance for particles (Massei, 2001; Massei et al., 2000, 2002). When considering

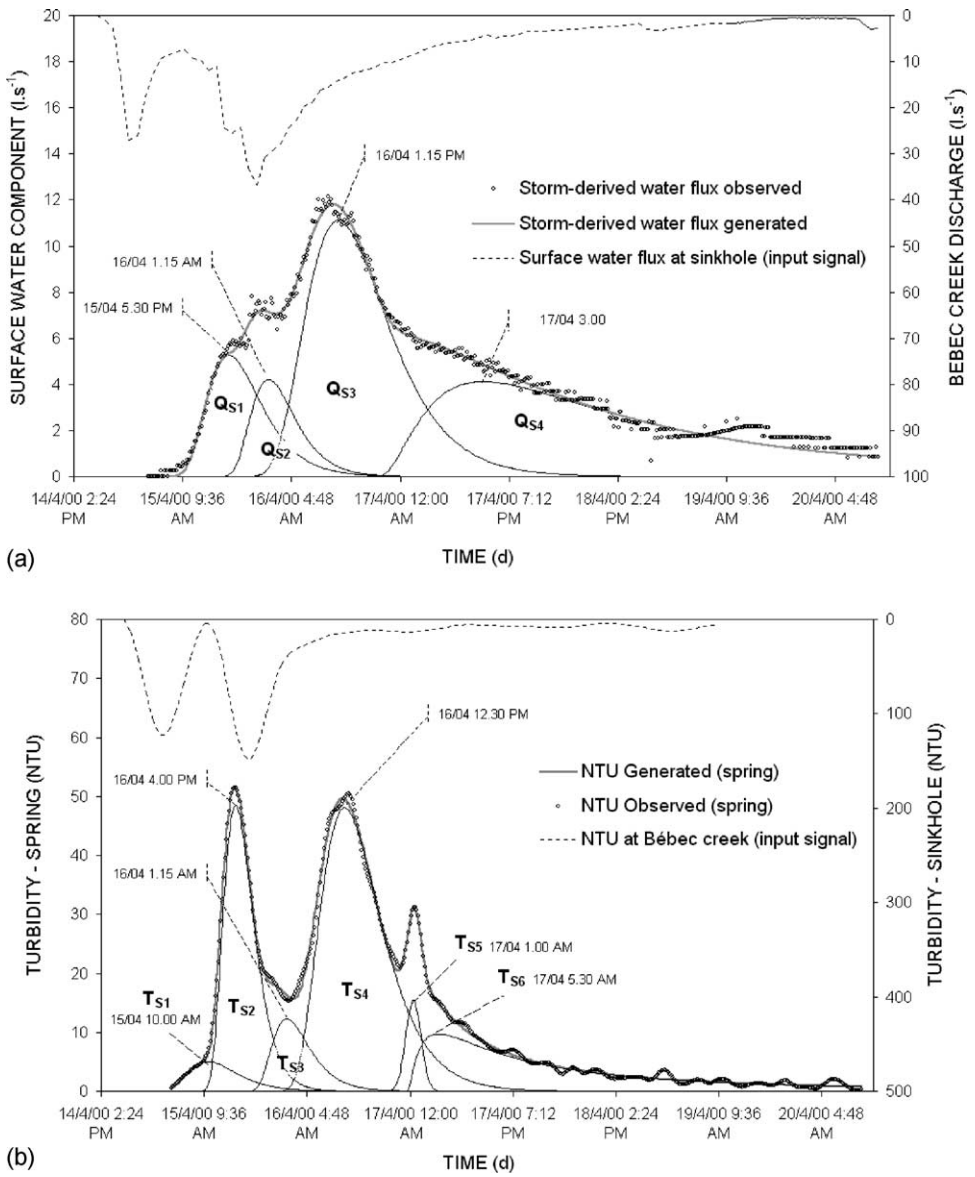

Fig. 7. Signal decomposition at the spring using the second-derivative method for: (a) storm-derived water; (b) particle breakthrough curve.

raw data only, the mass-balance is 51 ± 4%, with a swallowed mass of $6.29 \pm 0.20 \times 10^2$ kg and a recovered mass of $3.22 \pm 0.14 \times 10^2$ kg. The similarity of the transfer times of Q_{S1} and T_{S2}, Q_{S2} and T_{S3}, and Q_{S3} and T_{S4}, allows to deduce a direct transport of particles from the sinkhole to the spring for these T_{Si} peaks. On the other hand, according to this criterion, peaks T_{S1}, T_{S5}, and T_{S6} do not appear to be associated to a surface flux after decomposition of the global signal. We interpret these cases as resuspension phenomena of particles previously deposited within the karstic system. Thus, turbidigraph separation can be performed: the two components of particle transport (e.g. direct transfer and resuspension) can be quantified, as shown in Fig. 8 expressed as particle flux. So we can deduce that $2.35 \pm 0.14 \times 10^2$ kg out of $3.22 \pm 0.14 \times 10^2$ kg (total recovered mass)

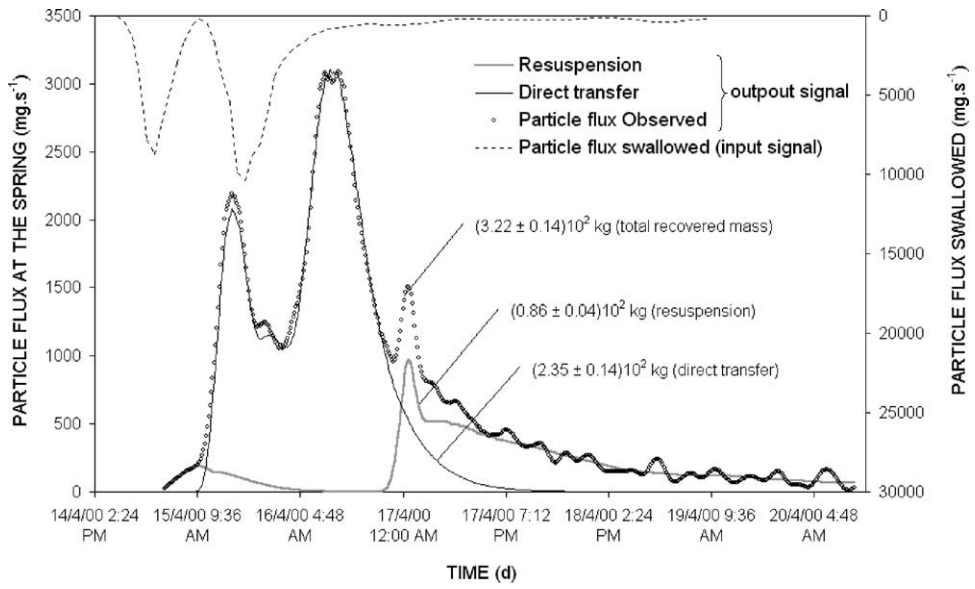

Fig. 8. Result of turbidigraph separation: reconstruction of direct transfer and resuspension components of the particle flux at the spring by summation of the elementary corresponding signals.

of solid materials would result from direct transfer (that is 73% of the total recovered mass), and $0.86 \pm 0.04 \times 10^2$ kg result from resuspension (that is 27% of the total recovered mass). A mass-balance of suspended particulate matters can be re-calculated, accounting for resuspended mass that we deduce from the total recovered mass: the corrected recovery rate, computed using the mass eluted by direct transfer solely (e.g. $2.35 \pm 0.14 \times 10^2$ kg), is $37 \pm 3\%$, instead of $51 \pm 4\%$ which was calculated from raw data.

According to relations between various signals Q_{Si} and T_{Si}, it is possible to make hypotheses on the origin of resuspension, whether resuspension is involved by aquifer global functioning or storm-derived water flux. Among signals attributed to resuspension, we observe that:

- T_{S1} precedes T_{S2} (which is characteristic of direct transfer) about 6 h in terms of transfer time: T_{S1} would then proceed from particle resuspension by pressure transfer consequently to injection of storm water at the sinkhole, rather than to an increase of the aquifer discharge, the latter being unobserved at this moment. These sediments would have been deposited consequently to a previous flood. Pressure transfer would occur once a hydraulic continuity is realized between the surface water introduction system and the saturated zone;
- T_{S5} is not related to a surface flux, as one can see in Fig. 7(a) and (b). It would correspond to the increase (rising limb) of the aquifer component of the total spring discharge (Fig. 5). The occurrence of this particle flux signal would be controlled by the global functioning of the aquifer consequently to the increasing hydraulic head in the saturated zone, rather than controlled by the dynamics of the introduction system (sinkhole subsurface introduction system);
- T_{S6} would originate from resuspension of previously deposited sediment, that may occur thanks to Q_{S4}. This last storm-derived water flux is not directly associated with turbidity input at the sinkhole. Actually, we can notice that on the plateau the recession of turbidity is faster than that of surface runoff (Fig. 7(a) and (b), dotted line), corresponding to a negligible particle transport at the end of runoff.

Resuspension of previously deposited particles can be so induced either by the dynamics of the introduction system, or by the global dynamics of the aquifer. In the first case, resuspension would be

induced by the occurrence of storm-derived water flux within the system, involving a reset in motion of previously deposited particles. In the second case, resuspension would be due to the dynamics of the karst aquifer, independently of that of the introduction system.

On a geomorphologic point of view, one can consequently make hypotheses on the location of the deposition zones: sediments corresponding to T_{S5} are not likely to originate from the input zone (introduction system), but rather directly from the main conduit, as T_{S5} corresponds to the contribution of the aquifer, rather then that of storm-derived water. In addition, the T_{S1} signal, which is characteristic of resuspension by pressure transfer, would be also related to sediment deposited within the saturated zone. One could then suppose that deposition takes place essentially in the main conduit flow system, rather than in the introduction system.

Particle breakthrough curve decomposition allows to distinguish two different functional/morphological parts of the system, that is, the introduction system and the conduit flow system.

4. Conclusion

This work demonstrates that the turbid response at karstic spring is rather complex, characterizing highly non-linear transport processes. The study also highlights the difficulty encountered to distinguish the part of resuspension of the particle flux measured at a spring. In the case of groundwater, the variations of water chemistry during a flood allow hydrograph separation. The difficulty to obtain relevant particle markers of residence times and deposition zones prevents a similar analysis of the transport processes of the solid phase in suspension. A fine comparison between hydrodynamics and particle transport, as presented in this paper, allows better understanding of the various processes, which control the occurrence of particle flux at karstic springs. Hydrograph separation by means of a two-component mixing model using corrected electrical conductivity allows to determine rather precisely the occurrence of turbidity with regard to hydrodynamics in the case of fairly simple binary karstic systems such as the one we studied. Actually, these relations remain imprecise if one considers only raw data. At the scale of the flood, peak detection using the second-derivative method, applied successively to the storm-derived water component and to particle breakthrough curve at a karstic spring, allows the comparison of elementary surface water flux and turbidity elementary signals in terms of transfer time. So it is possible to perform turbidigraph separation so as to distinguish the part of particle flux associated to direct transfer (e.g. allochthonous) from the part resulting from intrakarstic resuspension (e.g. resuspended). The mass-balance calculated from the allochthonous part only (e.g. involved by direct transfer) shows that the particle recovery rate previously calculated from raw data was overestimated. The fine time step (15 min) allowed by continuous measurements permits us to account for fine variations in the time-series which may be masked by larger time steps (≥ 1 h). Such fine variations provide a lot of important information about the nature and origin of transport processes. They also inform about the functioning and the structure of such karstic aquifers.

Acknowledgements

The authors would like to thank the Seine-Normandie Water Agency and the European Funding for Rural Development (EFRD) for the financial support. We also gratefully thank O. Atteia for his helpful comments and his interest in the paper.

References

Bakalowicz, M., 1979. Contribution de la géochimie des eaux à la connaissance de l'aquifère karstique et de la karstification. PhD Thesis, Université Paris 6, Moulis, 269 pp.

Beaudeau, P., Payment, P., Bourderont, D., Mansotte, F., Boudhabay, O., Laubiès, B., Verdière, J., 1999. A time series study of anti-diarrheal drug sales and tap-water quality. Int. J. Environ. Health Res. 9, 293–311.

Chatwin, P.C., 1971. On the interpretation of some longitudinal dispersion experiments. J. Fluid Mech. 48 (4), 689–702.

Coquerel, G., Lefebvre, D., Rodet, J., Staigre, J., 1993. La grotte du funiculaire (Le Mesnil sous Jumièges, Seine-Maritime): spéléogenèse et étude d'un remplissage ferro-manganique. Karstologia 22 (2).

Field, M., 2002. The Qtracer2 program for tracer breakthrough curve analysis for tracer tests in karstic aquifers and other

hydrologic systems. EPA/600/R-02/001, United States Environmental Protection Agency.

Lacroix, M., Leboulanger, T., Wang, H., 1998. Mise en évidence des relations surface-endokarst par la microgranulométrie, exemple du karst crayeux haut-normand. Bull. Soc. Geol. Fr. 169 (2), 177–187.

Lacroix, M., Rodet, J., Wang, H., Massei, N., Dupont, J., 2000. Origine des matières en suspension dans un système aquifère karstique: apports de la microgranulométrie. C. R. Acad. Sci., Paris, Série IIA 330, 347–354.

Laignel, B., Quesnel, F., Meyer, R., Bourdillon, C., 1999. Reconstruction of the upper cretaceous chalks removed by dissolution during the Cenozoic in the western Paris Basin. Int. J. Earth Sci. 88, 467–474.

Laignel, B., Quesnel, F., Meyer, R., 2002a. Classification and origin of the clay-with-flints of the western Paris Basin (France). Z.F. Geomorphol. 46 (1), 69–91.

Laignel, B., Spencer, C., Meyer, R., 2002b. The clay-with-flints of the western Paris Basin: a potential aggregate ressource. Environ. Geol. 41, 525–536.

Lautridou, J.P., 1985. Le cycle périglaciaire pléistocène en Europe du Nord-Ouest et plus particulièrement en Normandie. PhD Thesis, University of Caen, 908 pp.

Mahler, B., Lynch, F., 1999. Muddy waters: temporal variation in sediment discharging from a karst spring. J. Hydrol. 214 (1–4), 165–178.

Mahler, B., Bennett, P., Zimmerman, M., 1998a. Lanthanide-labeled clay: a new method for tracing sediment transport in karst. Ground water 36 (5).

Mahler, B., Winkler, M., Bennett, P., Hillis, D., 1998b. DNA-labeled clay: a sensitive new method for tracing particle transport. Geology 26 (9), 831–834.

Mahler, B., Lynch, F., Bennett, P., 1999. Mobile sediment in an urbanizing karst aquifer: implications for contaminant transport. Environ. Geol. 39 (1), 25–38.

Massei, N., 2001. Transport de particules dans l'aquifère crayeux karstique et à l'interface Craie/alluvions. PhD Thesis, Université de Rouen, Mont-Saint-Aignan, 195 pp.

Massei, N., Lacroix, M., Wang, H., Semega, B., Dupont, J., 2000. Transport of suspended solids through saturated porous media: experimental approach and field measurements. In: Sililo, O., (Ed.), Colloque IAH 2000, Groundwater: Past Achievements and Future Challenges, Balkema, Amsterdam, p. 5.

Massei, N., Lacroix, M., Wang, H., Mahler, B., Dupont, J., 2002. Transport of suspended solids from a karstic to an alluvial aquifer: the role of the karst/alluvium interface. J. Hydrol. 260 (1–4), 88–101.

Palmateer, G., MacLean, D., Kutas, W., Meissner, S., 1993. Suspended particulate/bacterial interaction in agricultural drains. S.S. RAO, 1–40.

Pinault, J., Plagnes, V., Aquilina, L., Bakalowicz, M., 2001. Inverse modeling of the hydrological and hydrochemical behavior of hydrosystems: characterization of karst system functioning. Water Resour. Res. 37 (8), 2191–2204.

Plagnes, V., 1997. Structure et fonctionnement de la zone noyée des karsts: caractérisation par la géochimie des eaux. PhD Thesis, Université Montpellier 2, Montpellier.

Pommepuy, M., Guillaud, J., Derrien, A., Le Guyader, F., Cormier, F., 1992. Enteric bacteria survival factors. Water Sci. Technol. 25 (12), 93–103.

Rodet, J., 1991. Les karsts de la craie: étude comparative. Paris IV (Paris-Sorbonne), 562.

Rodet, J., 1993. Le rôle des formations quaternaires dans le drainage karstique: l'exemple des craies du bassin de Paris. Quaternaire 4 (2–3), 97–102.

Rodet, J., 1996. Une nouvelle organisation géométrique du drainage des craies: le labyrinthe d'altération, l'exemple de la grotte de la Mansonnière (Bellou-sur-Huisne, Orne, France). C. R. Acad. Sci., Paris, Série IIA 322, 1039–1045.

Vaute, L., Drogue, C., Garrelly, L., Ghelfenstein, M., 1997. Relations between the structure of storage and the transport of chemical compounds in karstic aquifers. J. Hydrol. 199, 221–238.

Wicks, C.M., Engeln, J.L., 1997. Geochemichal evolution of a karst stream in Devils Icebox Cave, Missouri, USA. J. Hydrol. 198, 30–41.